JOURNAL OF AIRCRAFT
Vol. 38, No. 3, May–June 2001

Flow Separation Control with Microflexural Wall Vibrations

Sumon K. Sinha*
University of Mississippi, University, Mississippi 38677

A capacitively actuated active flexible wall (AFW) transducer has been developed for controlling boundary-layer flow separation. The transducer elements are first used as sensors to determine the most effective frequencies for wall actuation in the vicinity of a separating or marginally separated boundary layer. These frequencies typically result from an interaction of the flow with small-scale geometrical features of the wall. Microflexural vibratory actuation of selected regions of the transducer's flexible membrane at the aforementioned frequencies can then be used to defer separation as demonstrated in wind-tunnel experiments. The AFW transducer uses the preseparation velocity gradient at the point of actuation to amplify the microvibratory stimuli and cause it to modulate the pressure gradient. This subsequently promotes reattachment by enhancing mixing in the inflectional velocity profiles downstream. The high actuation efficiency and the ability to sense and actuate with the same hardware make the AFW transducer attractive for a wide range of practical aerodynamic problems for significantly extending the performance envelopes of fixed and rotary-wing aircraft and aircraft engines.

Nomenclature

C_D	=	coefficient of drag, $2F_D/(\rho DU_\infty^2)$ for cylinder and $2F_D/(\rho cU_\infty^2)$ for airfoil
C_p	=	nondimensional pressure, $2(p - p_\infty)/(\rho U_\infty^2)$
c	=	airfoil chord
D	=	cylinder diameter
F_D	=	drag force per unit span, N/m
f	=	transducer actuation frequency, Hz
h	=	wall normal distance from airfoil surface
p	=	local static pressure
p_∞	=	upstream static pressure
Re_c	=	Reynolds number for airfoil, $U_\infty \cdot c/\nu$
Re_d	=	Reynolds number for cylinder, $U_\infty \cdot D/\nu$
St	=	Strouhal number based on airfoil chord ($f \cdot c/U_\infty$) or cylinder diameter ($f \cdot D/U_\infty$)
St_s	=	Strouhal number based on s and U ($f \cdot s/U$)
s	=	characteristic length scale of near-wall geometrical features
T	=	membrane pretension per unit span, N/m
t	=	time
U	=	boundary-layer freestream velocity
U_∞	=	upstream velocity
u, v, w	=	local velocity components along x, y, and z directions
x, y, z	=	streamwise, wall-normal, and spanwise coordinates
α	=	airfoil angle of attack
δ	=	boundary layer thickness
θ	=	angular position from forward stagnation point on cylinder
μ	=	viscosity
ν	=	kinematic viscosity
ρ	=	density

I. Introduction

THE ability to coerce aerodynamic flows to follow the contour of a given lifting surface under adverse flow conditions plays an important role in extending the performance envelopes of fixed and rotary-wing aircraft and aeroengines. Boundary-layer flow separation can degrade the performance of an aerodynamic lifting surface in all flow regimes. For example, flow separation can degrade lift generation at low speeds and increase pressure drag at high speeds. Controlling flow separation in a simple and mechanically uncomplicated manner can open up new vistas for optimizing the design of wings. Weight savings from a simplified flap deployment mechanism, for example, can result in smaller wings and lower overall drag.

Simple passive devices, such as small surface-mounted vortex generators, can be used to extend the stall margin of a wing for low-speed, high-angle-of-attack operation. However, the same device will increase drag during high-speed, low-angle-of-attack operations. If both high-speed cruise as well as low-speed landing and takeoff performance have to be improved over a range of wing or blade loading conditions, active devices are required, which can be deployed or activated only when needed. Automatic activation and deactivation of such devices also necessitates some form of flow sensing. The role of an integrated sensor-actuator system is even more crucial if the flow separation is unsteady, such as the onset of dynamic stall[1] on rotorcraft blades or rotating stall[2] on axial compressor blades. The need for small lightweight devices makes microfabricated electromechanical systems or MEMS-based sensors and actuators especially suitable for such applications.

Minimizing device power consumption remains a prime consideration[3] for any active flow-separation control system. Hence, microactuators for flow control have usually been based on devices such as oscillating flaps[4,5] or periodically blown jets,[6,7] which are efficient in generating localized control vortices at selected regions in the boundary layer. However, the minimum actuation power needed is ultimately limited by the ability of the actuator to generate vortices strong enough for modifying the flow. For example, in periodic blowing the ratio of the jet momentum to the momentum of the freestream has to be above a certain threshold for maintaining control. Although the actuation power needed may be small in comparison to traditional techniques like steady streamwise blowing, it is often high enough to justify using less-than-optimum passive devices. Further reductions in actuator power consumption are possible only if the energy in the freestream can be used to efficiently amplify the actuation-induced control perturbations. This has been the motivation for developing the active flexible wall (AFW) transducer[8,9] described here. An additional motivation has been to make the device easy to integrate with existing designs without compromising structural integrity and without degrading the surface exposed to the flow.

Presented as Paper 99-3123 at the AIAA 17th Applied Aerodynamics Conference, Norfolk, VA, 28 June–1 July 1999; received 14 September 1999; revision received 28 June 2000; accepted for publication 8 September 2000.

*Associate Professor of Mechanical Engineering, 201-G Carrier Hall; mesinha@olemiss.edu.

The ability of passive compliant walls to modify boundary-layer flows has been known for some time,[10] although all possible modes of flow-wall interaction are not yet fully understood. Driven or AFWs offer the advantage of selectively energizing wall oscillation modes. Experiments have shown that flexural actuation of the wall at the correct frequency and phase can attenuate or reinforce Tollmien–Schlichting instability waves[11] on flat plates. However, similar experiments aimed at reducing flat-plate turbulent boundary-layer skin friction have not been as successful even after using fairly large wall displacement amplitudes.[12] An extension of the aforementioned techniques is the method postulated by Lurz.[13] It relies on introducing a combination of normal and tangential wall vibrations with the correct phase relationships to control transition, skin friction, and separation. The primary deterrent against practical implementation of these schemes is the difficulty in detecting phase relationships accurately in noisy "real life" flows. Hence, the flow-separation control scheme devised by Wygnanski,[7] which recommends the use of small oscillating flaps or flexible surface segments for actuation but does not require phase information, is clearly more practical.

The AFW transducer developed by Sinha[8] significantly reduces the actuation power needed for phase-independent oscillatory separation control by exploiting a unique combination of static and dynamic modes of flow-transducer interaction.[14] This paper is aimed at introducing this flow-separation control concept and discussing its significance to some current areas of interest in aerodynamics.

II. AFW Transducer

A. Construction of the AFW Transducer

Figure 1 shows a schematic of the AFW transducer array as used in proof-of-concept wind-tunnel experiments.[9] The transducer substrate consists of an array of strip-shaped electrical conductors. The substrate is typically etched out from a flexible copper-clad printed circuit board, the back side of which is glued on to the surface of the wing or blade as depicted in Fig. 2. A flexible dielectric membrane is stretched across the substrate. The outer surface of the membrane is metallized to make it electrically conductive and is exposed to the boundary-layer flow. Electrically, the membrane-substrate composite behaves as an array of capacitors. The conductive outer layer of the membrane constitutes one plate, which is shared by the capacitors. The conductive strips on the substrate form the other non-shared plates. The small air gap between the membrane and a strip establishes the capacitance and also contributes towards the flexural stiffness and damping of the membrane. A dc bias voltage helps maintain the air gaps by counteracting the lifting force induced by the external flow over the membrane.

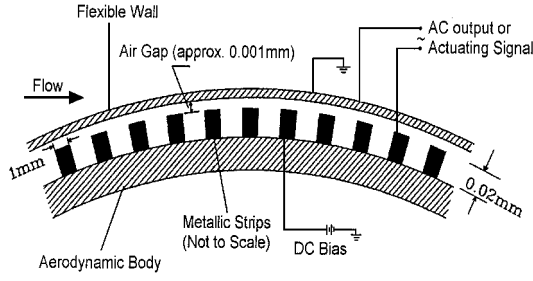

Fig. 1 Schematic of the AFW transducer.

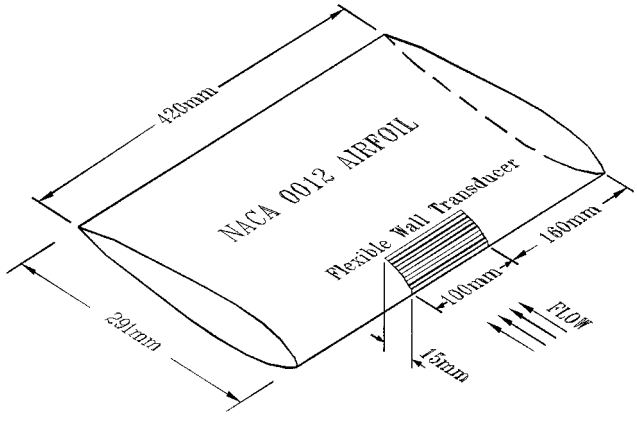

Fig. 2 AFW transducer mounted on an NACA 0012 airfoil model.

Each of the aforementioned capacitive transducers can behave as a sensor or actuator at any given instant. In the sensor mode flow-induced vibrations of the membrane above a conductive strip are sensed as voltage fluctuations resulting from changes in the thickness of the air-gap dielectric of the capacitor. In the actuator mode an external ac signal is used to electrostatically vibrate the segment of the flexible membrane above each strip. The amplitudes of displacement of the actuated membrane are typically in the order of 0.1 μm for strip widths between 0.4–1.6 mm. For the flow control experiments conducted with AFW transducers, membrane displacement amplitudes were at least three orders of magnitude smaller than the thickness of the boundary layer at the point of excitation.[9]

The control strategy involves using the transducer elements as on-line wall-pressure fluctuation sensors. The amplitudes of the signals from successive transducer strips can be compared to detect regions of incipient separation as described in Sec. III. The frequency spectrum of the signal from a strip in this region is then analyzed to identify the most effective frequency for flow-transducer interaction. Selected elements upstream of the separation point are then actuated at this frequency to reattach a separated flow or prevent an incipient separating flow from progressing to full breakaway separation. The details of the flow-transducer interaction are described in the subsequent sections.

B. Explanation of How the AFW Transducer Controls Separating Flows

The AFW transducer array falls into a category of techniques that interact with boundary-layer flows via oscillatory forcing. However, the mechanics of interaction is not the same, although some apparent similarities can exist.[14] To understand how an extremely small-amplitude motion of the membrane can control the flow, the streamwise momentum equation at the "wall" (i.e., the surface of the membrane at $y = 0$) is considered under excited conditions:

$$v\left(\frac{\partial u}{\partial y}\right)_{y=0} = -\left(\frac{1}{\rho}\right)\left(\frac{\partial p}{\partial x}\right) + \left(\frac{\mu}{\rho}\right)\left(\frac{\partial^2 u}{\partial y^2}\right)_{y=0} \tag{1}$$

The streamwise velocity component $u_{y=0}$ of the vibrating membrane has been assumed to be negligible. For a rigid nonporous wall the left-hand side of Eq. (1) is identically zero. For the driven flexible wall this represents the actuation or control term. The small wall-normal perturbation velocity of the membrane $[v_{y=0} = v_0 \cos(2\pi f t)]$ over an actuated strip can make this control term predominant provided $(\partial u/\partial y)_{y=0}$ is extremely large at the point of excitation. Such a condition can be satisfied at the leading edge of an excited strip as depicted in Fig. 3. If the control term is balanced primarily by the viscous term, large fluctuations in the streamwise velocity component u should be seen close to the wall. Figure 4 shows measured boundary-layer velocity fluctuation spectra in the vicinity of the point of actuation for AFW-actuated flow control experiments over a circular cylinder.[15] These indicate

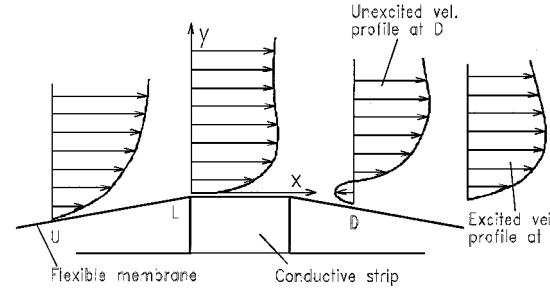

Fig. 3 Schematic showing near-wall flow-transducer interaction: U, point just upstream of conductive strip, and L, most effective point to introduce excitation.

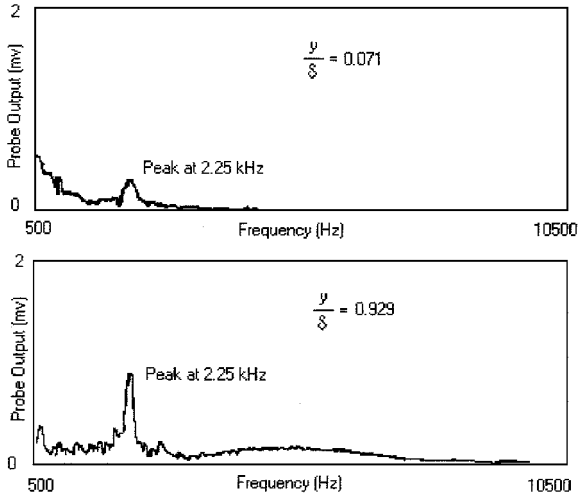

Velocity fluctuation spectra showing peaks at excitation frequency of 2.25 kHz

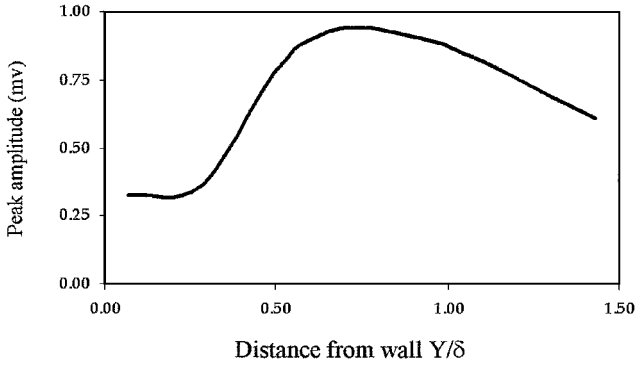

Variation of the 2.25 kHz peak with distance from wall

Fig. 4 Measured velocity fluctuation spectra at $\theta = 90$ deg in AFW excited (between 88–90 deg) boundary layer over a cylinder from Wang.[15]

that velocity fluctuations at the 2.25-kHz actuation frequency are low near the wall and maximize near the outer edge of the boundary layer, thereby invalidating the large viscous term assumption. Therefore, the pressure gradient term needs to balance the control term in Eq. (1), and the viscous term in Eq. (1) should be very small compared to the other terms. The pressure gradient $(\partial p/\partial x)$ also has to satisfy the inviscid momentum equation at the outer edge of the boundary layer:

$$\left(\frac{\partial U}{\partial t}\right) + U\left(\frac{\partial U}{\partial x}\right) = -\left(\frac{1}{\rho}\right)\left(\frac{\partial p}{\partial x}\right) \tag{2}$$

For an unexcited steady flow the convective term on the left-hand side of Eq. (2) will exactly balance the pressure gradient term. Wall actuation-induced fluctuations in $(\partial p/\partial x)$ will therefore induce fluctuations in U, at the actuation frequency f, primarily through the unsteady term $(\partial U/\partial t)$ in Eq. (2). This explains how balancing the control and pressure gradient terms in Eq. (1) can result in large velocity fluctuations at the outer edge of the boundary layer.

For the viscous term in Eq. (1) to be small, the near-wall velocity profile $u(y)$ should be approximately linear at the point of excitation. Such a condition can exist, for example, close to the maximum thickness region of a streamlined body, where the pressure gradient $\partial p/\partial x$ passes through zero as it changes from favorable (i.e., negative $\partial p/\partial x$ upstream) to adverse (i.e., positive $\partial p/\partial x$ downstream). Because boundary-layer separation can occur only in the positive $\partial p/\partial x$ region, the optimum point of excitation would always be upstream of the unexcited flow-separation point.

The aforementioned actuation sequence results in the generation of coherent oscillatory flow structures, which are convected downstream by the flow. These can enhance mixing in shear-layer-like (SLL) structures within the boundary layer as verified by Sinha and Pal.[16] The SLL structures arise as a result of inflectional velocity profiles resulting from the adverse pressure gradient typical of separating boundary layers. Enhancing mixing in these shear layers therefore reenergizes the wall layer and delays or defers boundary-layer separation.

Typically, only one or two strips of the AFW transducer array need to be actuated for flow-separation control.[9] This, along with the extremely small membrane vibration amplitudes, helps in keeping the actuation power extremely low (typically less than 1 μW per meter span for freestream velocities between 15–50 m/s). The residual roughness and membrane compliance have imperceptible effects on the boundary layer for a "properly designed" AFW transducer. A proper design can be ensured by limiting the passive compliance and magnitudes of sharp changes in membrane slope as shown in Fig. 3. This is achieved by 1) limiting strip spacing and width, and by 2) pretensioning the membrane.[14] The sharp corners of the stretched membrane shown in Fig. 3 can also induce inflectional velocity profiles close to the wall similar to Falkner–Scan flows over expanding corners.[17] Such Falkner–Scan flows are known to have multiple solutions. Hence, it seems plausible that these also play a role in transferring kinetic energy between the vibrating membrane and the flow. However, the generation of vorticity as a result of actuation-induced changes in membrane slope is several orders of magnitude lower compared to wall vorticity generation by microflaps or oscillatory blowing.[4–6] The most effective control frequencies for the AFW transducer are also at least an order of magnitude higher[9] than other forms of separation control via oscillatory forcing. As described in Sec. III, these coincide approximately with vortex shedding frequencies corresponding to the near-wall geometrical features,[14] such as the spacing of sharp corners shown in Fig. 3. Control efficacy drops if these also coincide with the fundamental flexural natural frequency of the membrane[18] as described in Sec. III.B. The efficacy drops because the resulting resonance enhances additional vibrational modes of the membrane. These eventually diffuse the localized effect of actuation, thereby destroying the required balance between terms in Eq. (1).

III. Experimental Verification of Flow-Separation Control

A. Flows over Cylinders

The AFW flow-separation control concept has been validated through proof-of-concept experiments on circular cylinders and airfoils. The experiments have involved sensing and actuation in steady and unsteady flows. Figure 5 shows a typical spectrum of the sensed signal from a transducer strip for crossflow over a circular cylinder.[9,15] The broadband peak at 2.25 kHz was the most effective excitation frequency in this case. Excitation of two transducer strips upstream of the separation point moved the separation point downstream as seen from the measurement of time-averaged pressures around the cylinder in Fig. 6. A smoke visualization of the flow in

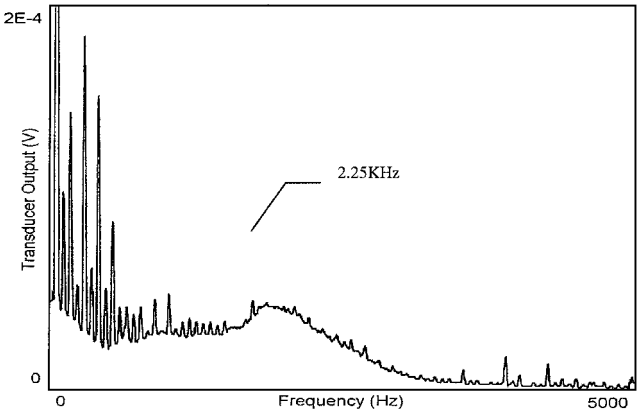

Fig. 5 Spectrum of signal from AFW transducer at 78 deg (unexcited flow over cylinder at $Re_d = 1.5 \times 10^5$).

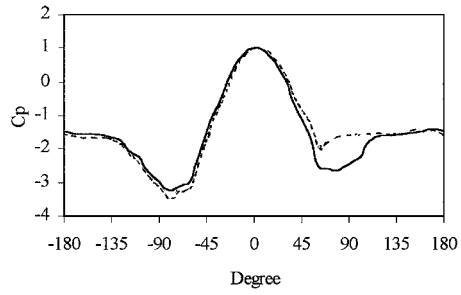

Fig. 6 Pressure distribution over cylinder (AFW excited at $\theta = 88$–90 deg at 2.25 kHz): - - - -, unexcited, and ——, excited.

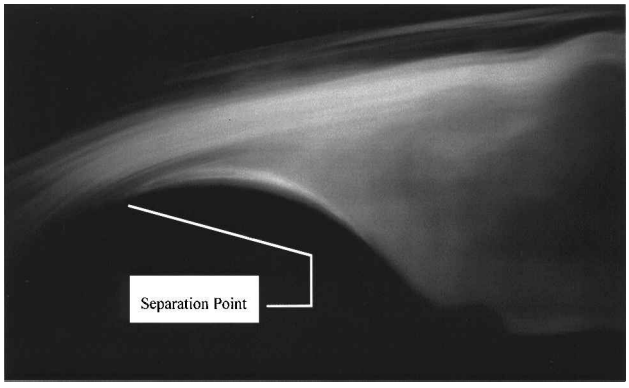

Unexcited flow

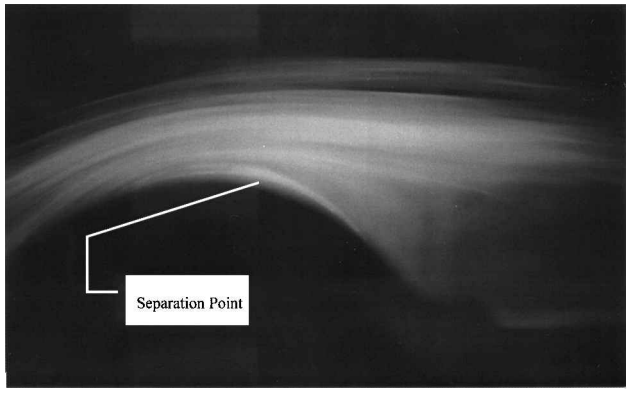

Excited flow

Fig. 7 Flow visualization results for flow over cylinder at $Re_d = 1.5 \times 10^5$.

Fig. 7 clearly shows a bending of the freestream flow toward the wall resulting from excitation. The asymmetry in the pressure distribution over the cylinder for the unexcited flow (Fig. 6) shows the presence of some passive interaction with the flow since. Even though the effect of such interaction is small, communication through the rounded trailing edge of the cylinder and the relatively high (i.e., 25%) blockage caused by the presence of the cylinder accentuated the flow asymmetry. Actuating the AFW transducer resulted in reducing the drag by 12.4% and the drag-induced power loss by about 300 W/m span while the electrical actuation power remained less than 0.5 μW per meter span of the cylinder. The Strouhal number ($St = f D/U_\infty$) or nondimensional excitation frequency was about 23 for this case. This is high compared to values of the order unity for separation control by other forms of oscillatory forcing (e.g., oscillatory blowing) for similar flows. An additional effect of AFW excitation was the suppression of low-frequency ($St \approx 0.2$) vortex shedding from the cylinder.[9] Vortex shedding, or the underlying frequency, has no bearing on the flow control process because the optimum excitation frequency and control efficacy remained virtually unchanged even after a splitter plate was used to attenuate vortex shedding.[15] Also, the separation point could be made to switch back and forth by periodically commencing and turning off the actuating signal to the AFW transducer.

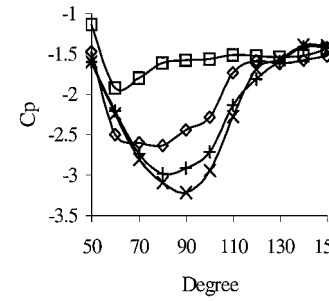

Fig. 8 Close up of pressure distribution on cylinder (AFW excited at 2.25 kHz, $Re_d = 1.5 \times 10^5$, hump at $\theta = 88$ deg): □, without hump, unexcited; ◇, without hump, excited; |, with hump, unexcited; and ×, with hump, excited.

The aforementioned experiments, which were conducted at $1.2 \times 10^5 < Re_D < 1.5 \times 10^5$, indicated that the AFW transducer worked most effectively for laminar flows close to transition. Was the transducer simply tripping the boundary layer? Exciting a turbulator-strip tripped flow showed improved pressure recovery and a 20% reduction in drag and C_D compared to tripped but unexcited conditions.[9] Although turbulators and AFW excitation have similar effects on separation delay, the effect on flow turbulence levels is markedly different. Unlike turbulators, AFW excitation has been found to reduce turbulence levels in the boundary layer and wake in all cases. Both methods, however, increase the mean velocities near the wall. The synergism improved when the preseparation velocity profile was preshaped, without tripping, with a shallow wall-mounted hump.[15,19] Figure 8 shows the enhancement in pressure recovery afforded by the hump and AFW excitation individually and in unison. In all cases the maximum boundary layer and wake turbulence levels increased if the shape or size of the bump or distributed roughness elements extended beyond a certain threshold. A properly applied (see Sec. II.B) unexcited AFW transducer, however, did not increase the turbulence levels measurably compared to the base flow on the rigid cylinder.

B. Flows over Airfoils

Exploratory wind-tunnel studies[20] showed the transducer capable of reattaching marginally separated flows around the leading edge of an NACA 0012 airfoil for $4 \times 10^5 < Re_C < 1 \times 10^6$. Independent (unpublished) airfoil experiments by Professor Lorne Whitehead at the University of British Columbia, Canada, showed lift enhancement, stall delay, and reduction in flow unsteadiness using a similar transducer. Many of these results, however, have been difficult to replicate until a method to precisely control the pretension of the flexible membrane of the transducer was devised. The tension is a key factor in establishing the predominant flexural modes of the membrane.[14,18] Figure 9 shows sensed signals from a 0.4-mm wide leading-edge AFW transducer strip on an NACA 0012 airfoil. For these experiments the membrane pretension was held at 92 N/m, and the airfoil was set at an angle of attack $\alpha = 14$ deg. The 92 N/m tension level ensured that the natural frequencies for the fundamental and second higher flexural modes of the membrane segment between two strips straddled the most effective actuation frequencies for control. In Fig. 9 the natural frequencies of the membrane segments are seen as sharp peaks that do not change with flow velocity, whereas the flow-induced excitation frequency increases with the flow velocity. The latter, which correspond to $St \approx 200$, have been found to be the optimum frequencies for flow separation control. Also, several closely spaced peaks are observed when the two frequencies coincide, indicating the onset of additional vibrational modes of the membrane.

The effect of AFW actuation on flow separation was ascertained by monitoring the velocities at a fixed point just above the suction surface of the airfoil as shown in Fig. 10. At low Re_c values complete breakaway separation occurs from the airfoil leading edge, and AFW

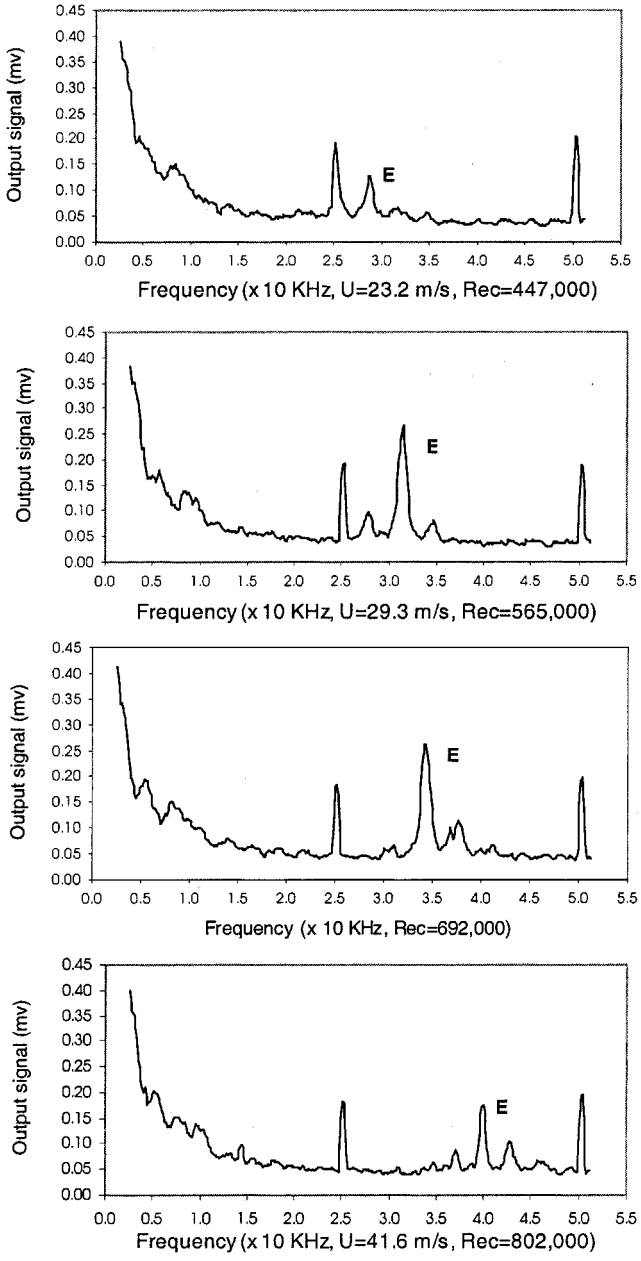

Fig. 9 Sensed signals on NACA 0012 airfoil set at 14 deg angle of attack (*E*-the most effective frequency for control).

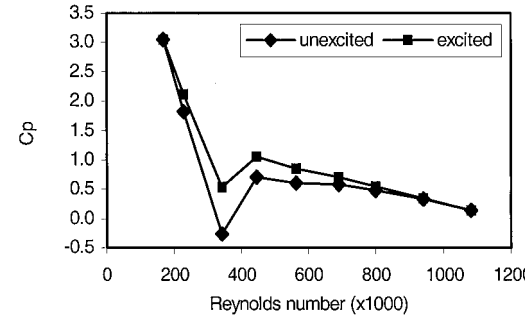

Fig. 10 Effect of AFW excitation at optimum frequencies on NACA 0012 airfoil between $0 < x/c < 0.05$ for 14 deg, velocity measured at $x/c = 0.5$, $h/c = 0.01$ (h is the distance from surface).

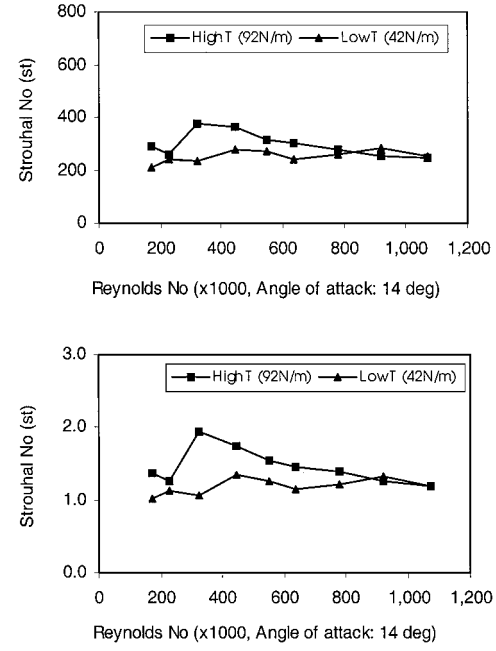

Fig. 11 Optimum excitation Strouhal numbers for NACA 0012 airfoil. (top: *St*; bottom: St_s)

actuation is ineffective. Hence, the actuation-induced increases in velocity also diminish there. The effect of excitation maximizes around $3 \times 10^5 < Re_c < 5 \times 10^5$ because of an excitation-induced reduction in size of the separation bubble. At higher Re_c values the effects of AFW actuation diminishes because the unexcited boundary layer was still attached at $\alpha = 14$ deg. The effect of AFW actuation maximized for the marginally separated cases corresponding to $\alpha = 14$ deg. Figure 11 shows the optimum excitation frequency f based Strouhal number ($St = fc/U_\infty$) as a function of Re_c for two different membrane pretension levels. In both cases St converges to about 230 as Re_c increases beyond 5×10^5. To understand the origin of such a high optimum excitation frequency, the Strouhal number is redefined as $St_s = f.s/U$, where s is an appropriate scale of near-wall geometrical features and U is the boundary-layer freestream velocity in the vicinity of the point of actuation. For the experiments described in Fig. 11, $U \approx 2U_\infty$, and $s = 2$ mm corresponding to the center-to-center distance of the transducer strips. These yield a St_s value around 1.5, which is of order one. This confirms the role of near-wall small-scale geometrical features in AFW flow control. The significance of $St_s \sim \mathcal{O}(1)$ is that it represents a situation where the actuation-induced pressure fluctuations above a strip are in phase with the pressure fluctuations induced by the motion of the membrane above the strip immediately downstream as long as the convection velocity corresponds to U (i.e., approximately the velocity of the layer where velocity fluctuations at the excitation frequency maximize as shown in Fig. 4). In all of the flow control experiments, exciting two adjacent strips in phase at the aforementioned optimum frequencies either improved the control effect or left it unchanged. The wall scale s can be modified if a separation bubble exists near the point of actuation, or if the pretension T is insufficient for holding the membrane in close proximity with the transducer substrate. This shows up as the anomalous behavior of the curves in Fig. 11 around $3 \times 10^5 < Re_c < 5 \times 10^5$.

IV. Practical Applications

Based on an understanding of how the transducer controls the flow, several practical uses can be envisioned as outlined in Table 1. To exploit the unique microvibratory actuation mechanism, applications need to be restricted to situations where 1) marginal separating conditions can be ensured at least locally and 2) suitable locations for actuation exist immediately upstream of the separation point where the near-wall velocity gradient is approximately linear. Existing data on cylinders and airfoils clearly demonstrate the capability of the AFW transducer for controlling both steady and unsteady separating flows. However, the system architecture for on-line control of unsteady separation can be expected to be significantly more complex.

Table 1 Possible applications of the AFW transducer

Application	Estimated performance enhancement	Basis for estimate
Drag reduction through enhanced pressure recovery on NLF wing	2–5% drop in drag	Preliminary flight tests
Stall detection and control on fixed wing aircraft 1) on main wings 2) on flap leading edges 3) on leading edges of vertical and horizontal stabilizers	Increase stall angle by 5 deg and $C_{L\text{-Max}}$ by 10% at low Reynolds numbers. Also reduce flow unsteadiness by 50% or more	Wind-tunnel experiments on statically stalled wings
Detection of incipient unsteady separation on rotorcraft blades followed by control	Safety enhancement by detecting edge suction precursors to leading-edge suction-peaks and delaying their occurence	Wind-tunnel experiments on pitching wings
Delaying the onset of unsteady separation on dynamically stalled blades and wings	Increase stall angle and $C_{L\text{-Max}}$ at low to moderate Reynolds numbers and rapid pitch rates	Wind-tunnel experiments on pitching wings
Separation control on turbine-engine axial compressor blades (stators and rotors) and engine inlets	1) Control the onset of rotating stall. 2) Increase stage pressure ratios by 10% without increasing bleed flow rates	Unsteady separation control experiments for flows over a cylinder
Control aeroelastic instabilities by adaptively controlling structural vibration-induced incipient separation	Structures can be made lighter. Can also be used to reduce noise and improve efficiencies of propellers and fan blades	Unsteady separation control experiments for flows over cylinders and airfoils
Reduce parasitic drag and vortex shedding	Reduce drag by 20% and eliminate large-scale unsteadiness	Unsteady separation control experiments for flows over cylinders
Fluidic amplification device for large-amplitude low-frequency perturbations by modulating the actuation signal	1) Nozzle thrust vectoring 2) Enhanced fuel-air mixing in combustors 3) Jet noise reduction 4) Aerodynamic directional control	Unsteady separation control experiments for flows over cylinders

A. Preliminary Flight Tests

In view of the aforementioned considerations, one of the first practical cases being investigated is using the transducer to reduce cruise drag on an advanced natural laminar flow (NLF)-0414F airfoil.[21] Typically, the extremely low-drag characteristics of NLF airfoils suffer as a result of deviations in wing loading and speed from ideal design conditions. The thicker-than-ideal wake results from an existence of marginally separated flow near the trailing-edge pressure recovery region. To investigate the effectiveness of the AFW transducer in enhancing pressure recovery in such situations, exploratory flight tests were conducted. An AFW transducer having a 300-mm spanwise and 50-mm chordwise active region was mounted on the lower surface of a 1.3-m chord NLF-0414F wing of an experimental Global GT-3 trainer. The transducer array was centered 71% from the leading edge. Sublimation tests on the wing indicated a laminar-turbulent transition location between 50–60% of the chord on the lower surface. Figure 12 shows typical measured lower surface wing boundary-layer velocity profiles 74% from the leading edge corresponding to a 55-m/s constant speed level flight of the aircraft. The velocity profiles were measured with a wing-mounted boundary-layer total-head tube rake connected to an array of individually calibrated pressure transducers. The individual tube measurements had a $\pm 0.1\%$ uncertainty. Exciting a 0.4-mm-wide transducer strip located 68.2% of the chord behind the leading edge at 20-kHz increased the velocities in the boundary layer as shown in Fig. 12. The corresponding momentum increase, estimated by numerically integrating the velocity profiles, indicated a drag reduction of 2.7%. Turbulent fluctuations in the atmosphere can significantly affect flight-test results by altering the base flow conditions during the time interval between acquiring data for excited and unexcited conditions. Earlier tests with a traversing wing-wake velocity probe displayed about 1% drag reduction[22] but showed large fluctuations. Therefore, the present boundary-layer rake measurements were repeated such that the unexcited and AFW-excited boundary-layer velocity profiles were recorded in quick succession during the same constant-speed pass. An analysis of these test data revealed an average increase in the momentum flux (i.e., ρu^2) of at least 2% with a 97% level of significance. The optimum excitation frequency of 20 kHz corresponded to $St = 478$ and $St_s = 6$. Halving the excitation frequency to 10 kHz also indicated some drag reduction. However, the effect disappeared at the intermediate frequency of 15 kHz. This supports the explanation offered in Sec. III.B about the relevance of $St_s \sim \mathcal{O}(1)$.

The preceding results show that by applying the transducer to both upper and lower surfaces of an NLF wing a potential for 2–5% drag reduction exists. The advantage of using the AFW transducer array for this application is that the location and frequency of actuation can be changed according to wing loading, flight altitude, and speed. This information can be stored in a look-up table, thereby simplifying the control system architecture.

B. Additional Considerations for the AFW Transducer

1. *Transducer Configuration*

The construction of the flexible-wall transducer, as shown in Fig. 1, suffers from certain intrinsic drawbacks. The discussions in this section pertain to design modifications aimed at removing these. The first problem is that the thin air gap between the flexible membrane and conducting-strip substrate needs to be controlled closely. Because the gap is influenced by a balance between the electrostatic attraction and local flow-induced suction, the maximum allowable velocity for a particular application can be expected to be a function of the breakdown voltage of the dielectric membrane/air-gap combination. This problem can be alleviated by pretensioning the membrane mechanically, such that the tension maintains the gap when the transducer is applied to a convex surface. However, if the gap becomes too small actuation amplitudes are constrained. This can be circumvented by using varying height strips. The membrane typically rests on the tall strips. The difference in heights between the tall and short strips sets the air gap.

A simplified dynamic model of the transducer[23] indicated that actuation efficacy increases with a reduction in strip width. Thus, reducing strip widths from 1 mm down to perhaps 30 μm through microfabrication will definitely be beneficial. An additional benefit of reducing strip width is the improvement in efficacy afforded by an ability to introduce the actuation more accurately with respect to the flowfield. This can be expected to be crucial for leading-edge separation control on thin airfoils, which have large streamwise variations in the pressure gradient.

2. *Transducer Materials*

The material of the flexible membrane needs to be chosen carefully because it not only has to be sufficiently flexible and light, but also has to have the requisite dielectric properties and resistance to degradation from exposure to the environment. A study by Laird[24] recommended a composite consisting of a base layer of dielectric rubber coated with a thin layer of aluminum and topped off with a thin layer of polyethyleneterepthalate (PET or Mylar) as the material for the membrane for external aerodynamic applications. PET films are not subject to degradation by ethylene glycol, a commonly used deicing fluid and are not degraded by UV light. The PET constrains

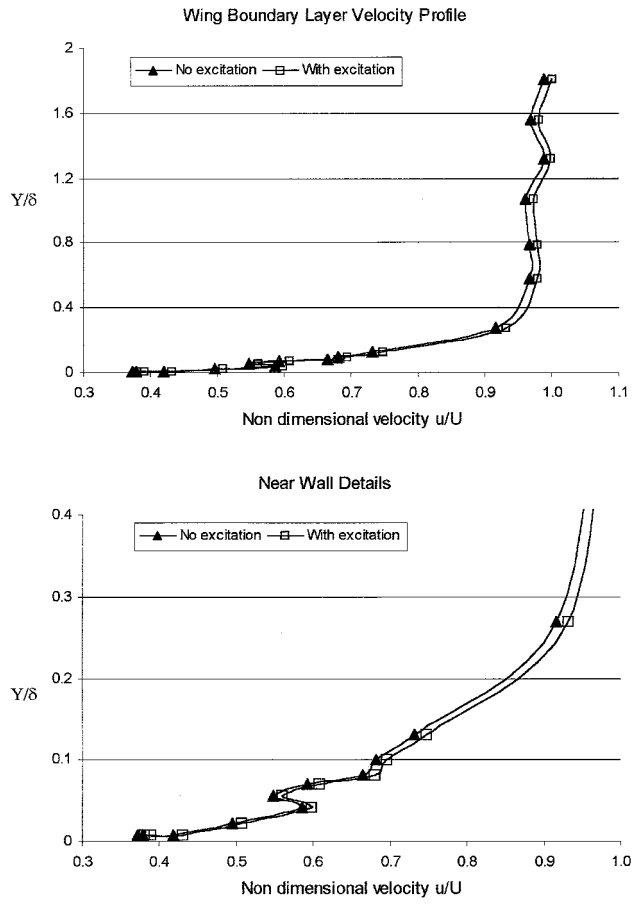

Fig. 12 Velocity profile downstream of AFW transducer mounted on lower surface of NLF-0414F wing of global GT-3 test aircraft ($Re_c = 4.8 \times 10^6$). Strip at $x/c = 0.68$ excited at $f = 20$ kHz, or $St = 478$, or $St_s = 6$.

the useful operating temperatures between −40–115°C. The rubber, although susceptible to UV degradation, is shielded by the metallic layer in this configuration. Additionally, the rubber can have a system of microstructured grooves in order to customize the effective damping and compliance of the transducer.[25]

3. *Control System Architecture*

If the AFW transducer is used to control steady or quasi-steady separation processes, the sensing feature of the transducer elements will only be needed to establish the criteria for excitation. A simple open-loop control can be used as outlined in Sec. IV.A. For on-line separation control, however, the control architecture for this device needs to be somewhat unique because the same transducer elements serve as sensors as well as actuators. The controller has to keep track of the mode of each transducer element, deduce the possibility of an upcoming flow separation, and actuate the appropriate strips to defer it. Although this may present itself as a formidable problem, it is expected to be significantly less complex compared to using sensor-actuator systems for turbulent skin-friction reduction through the mitigation of ejections and sweeps. First, only one or two strip-shaped transducer elements need to be used as actuators at any given instant. Second, it may be possible to simplify the separation detection process into a few simple steps, each requiring data from a limited number of sensors. For example, it has been observed from experiments on pitching airfoils that wall-pressure fluctuation amplitudes increase substantially as the separation point is approached both in space and time.[26] This can be used to focus attention on perhaps 4–10 sensor strips in the neighborhood of the separation point. Finally, a neural net can be trained to predict the appropriate actuation frequencies, amplitudes, and locations from the data.

V. Concluding Remarks

A capacitively actuated AFW transducer has been developed for controlling aerodynamic boundary-layer flow separation. The transducer consists of a flexible membrane stretched over an array of strip-shaped electrodes. The interaction between the separating boundary-layer flow and the flexible membrane is different from other oscillatory flow control devices because it utilizes a flowfield-induced amplification of the microscale actuation of the membrane. The velocity profiles and pressure distributions have to meet fairly stringent requirements for the AFW transducer to be effective. The most effective frequencies for control are also considerably higher compared to oscillatory blowing or oscillating microflaps. For the AFW transducer these coincide approximately with vortex shedding frequencies corresponding to the near-wall geometrical features corresponding to $St_s \sim O(1)$. Control efficacy drops if these also coincide with the natural frequencies of the membrane corresponding to the most energetic flexural modes. Hence, designing the transducer for a particular application involves selecting the proper combination of membrane tension and strip spacing on the substrate.

Proof-of-concept wind-tunnel and flight experiments have shown that the AFW transducer can control steady and unsteady separating flows over cylinders and airfoils. The power consumption for actuating the transducer is very small. The transducer can work for transitional to turbulent flows as long as the conditions for actuation are met. For turbulent flows AFW actuation is most effective when introduced during the transition process. Exciting the transducer in this manner modifies the boundary-layer flow structure by increasing the mean velocities while reducing overall turbulence levels. Although it is possible to use this transducer for real-time control of unsteady separating flows by combining the sensing and actuating functions, the control system architecture can be greatly simplified for situations when real-time control is not needed. Additionally, the compatibility of the transducer materials with the operating environment has to be ensured.

Acknowledgments

Support from the U.S. Army Research Office through Grant DAAG55-98-1-0243, monitored by Thomas Doligalski, is gratefully acknowledged. The author acknowledges the National Science Foundation for sponsoring the flight tests through an SBIR Phase-1 Grant (Award Number 9961054) to Global Aircraft Corporation, Starkville, Mississippi, and Michael R. Smith of Global Aircraft for providing the test aircraft and instrumentation and conducting the flight tests. The author would also like to thank his colleagues Shyam N. Prasad, Professor of Civil Engineering, and John A. Fox, Emeritus Professor of Mechanical Engineering, for critiquing the work and providing valuable suggestions.

References

[1] Carr, L. W., "Progress in the Analysis and Prediction of Dynamic Stall," *Journal of Aircraft*, Vol. 25, No. 1, 1988, pp. 6–17.

[2] Cohen, H., Rogers, G. F. C., and Saravanmuttoo, H. L. H., *Gas Turbine Theory*, 4th ed., Longman Group, Ltd., Essex, U.K., 1996.

[3] Gad-el-Hak, M., and Bushnell, D. M., "Separation Control: Review," *Journal of Fluids Engineering*, Vol. 13, No. 1, 1991, pp. 5–30.

[4] Ho, C. M., and Tai, Y. C., "Micro-Electromechanical Systems (MEMS) and Fluid Flows," *Annual Review of Fluid Mechanics*, Vol. 30, 1998, pp. 579–612.

[5] Seifert, A., Eliahu, S., Greenblatt, D., and Wygnanski, I., "Use of Piezoelectric Actuators for Airfoil Separation Control," *AIAA Journal*, Vol. 36, No. 8, 1998, pp. 1535–1537.

[6] Seifert, A., Darabi, A., and Wygnanski, I., "On the Delay of Airfoil Stall by Periodic Excitation," *Journal of Aircraft*, Vol. 33, No. 4, 1996, pp. 691–699.

[7] Wygnanski, I., "Method and Apparatus for Delaying the Separation from a Solid Surface," U.S. Patent 5,209,438, May 1993.

[8] Sinha, S. K., "System for Efficient Control of Separation Using a Driven Flexible Wall," U.S. Patent 5,961,080, Oct. 1999.

[9] Pal, D., and Sinha, S., "Controlling Unsteady Separation on a Cylinder with a Driven Flexible Wall," *AIAA Journal*, Vol. 36, No. 6, 1998, pp. 1023–1028.

[10] Bushnell, D. M., Hefner, J. N., and Ash, R. L., "Effect of Compliant Wall Motion on Turbulent Boundary Layers," *Physics of Fluids*, Vol. 120, No. 10, Pt. 2, 1977, pp. S31–S48.

[11]Wehrmann, O. H., "Tollmien-Schlichting Waves Under the Influence of a Flexible Wall," *Physics of Fluids*, Vol. 8, July 1965, pp. 1389, 1390.

[12]Weinstein, L. M., "Effect of Driven Wall Motion on a Turbulent Boundary Layer," *Proceedings of the IUTAM Symposium on Unsteady Turbulent Shear Flows*, Springer-Verlag, 1981, pp. 58–66.

[13]Lurz, W., "Method and Apparatus for Controlling the Boundary Layer Flow over the Surface of a Body," U.S. Patent 4516747, May 1985.

[14]Sinha, S. K., Wang, H., and Zou, J., "Interaction of an Active Flexible Wall with Separating Boundary Layers," AIAA Paper 99-3594, June–July 1999.

[15]Wang, H., "Flow Separation Control with an Active Flexible Wall," M. S. Thesis, Mechanical Engineering Dept., Univ. of Mississippi, University, MS, May 1998.

[16]Sinha, S., and Pal, D., "On Controlling Flow Separation with a Driven Flexible Surface," *Proceedings of the Seventh Asian Congress of Fluid Mechanics*, Vol. I, Allied Publishers, New Delhi, India, Dec. 1997, pp. 323–326.

[17]Schlichting, H., *Boundary Layer Theory*, 7th ed., McGraw–Hill, New York, 1979, pp. 150, 151.

[18]Pal, D., Sinha, S. K., Wang, H., Zou, J., and Chen, J., "Characterization of a Flexible Wall Sensor for Boundary Layer Pressure Fluctuation Measurements," AIAA Paper 99-0389, Jan. 1999.

[19]Sinha, S. K., and Wang, H., "Improving the Efficacy of an Active Flexible Wall for Controlling Flow Separation," AIAA Paper 99-0923, Jan. 1999.

[20]Banerjee, D., "An Experimental Investigation of Flow Separation Control Using an Acoustic Active Surface," M.S. Thesis, Mechanical Engineering Dept., Univ. of Mississippi, University, MS, Aug. 1995.

[21]McGhee, R. J., Viken, J. K., Pfenninger, W., and Beasley, W. D., "Experimental Results for a Flapped Natural Laminar Flow Airfoil with High Lift/Drag Ratio," NASA TM-85788, May 1984.

[22]Sinha, S. K., "Active Flexible Walls for Efficient Aerodynamic Flow Separation Control," AIAA Paper 99-3123, June–July 1999.

[23]Pal, D., "Mechanisms for Energy Transfer Between an Acoustically Active Compliant Wall and a Separating Boundary Layer," Ph.D. Dissertation, Univ. of Mississippi, Dept. of Mechanical Engineering, University, MS, May 1997.

[24]Laird, P., "Practical System for Commercial Aircraft Drag Reduction Using an Elastomeric Compliant Wall Active Multi-Element Array," Engineering Physics Thesis, Queen's Univ. at Kingston, Dept. of Physics, Ontario, Canada, June 1998.

[25]Whitehead, L. A., Clark, R. L., and Curzon, F. L., "Elastomer Membrane Enhanced Electrostatic Transducer," U.S. Patent 4,885,783, Dec. 1989.

[26]Sinha, S. K., Pandey, M., Wang, H., and Pal, D., "Using an Array of Transducers Under a Compliant Wall to Detect and Control Dynamic Stall on a Pitching Airfoil," AIAA Paper 98-0678, Jan. 1998.